

FSU-HEP-930609

hep-ph/9307238

June 1993

Measuring the Longitudinally Polarized Proton Gluon Distribution using Photoproduction Processes

S. Keller and J. F. Owens

*Department of Physics, B-159
Florida State University
Tallahassee, Florida 32306*

Abstract

Little information is known about the polarization of gluons inside a longitudinally polarized proton. We investigate the sensitivity of photoproduction experiments with both beam and target longitudinally polarized to the polarization of the gluon distribution in the proton. We study the photoproduction of jets and heavy quarks and conclude that they are both sensitive to the gluon polarization.

1. Introduction

Since the so-called EMC spin crisis has emerged[1, 2], much theoretical work has been done[3]. Central to the debate is the size of the gluon polarization inside a longitudinally polarized proton. The only information available about the gluon polarization is given through higher order corrections to spin-dependent structure functions or through its effect on the evolution of polarized quark distribution functions. However by considering reactions for which the gluon plays a role at leading order, the sensitivity to its polarization will be increased. Many ways to measure the gluon polarization in this more direct fashion have been suggested in polarized deep inelastic scattering[4, 5, 6] and polarized hadron-hadron interactions[7]. In this paper, the sensitivity to the gluon polarization is studied in photoproduction experiments where both the photon and the proton are longitudinally polarized. The production of both jets and heavy quarks is considered. Although these processes have been studied before[8, 9], they are reconsidered here in more detail and in light of a possible large gluon polarization.

In Section 2, leading order sets of polarized distribution functions compatible with the EMC result and the work of Bodwin and Qiu[10] are presented. Different amounts of gluon polarization are considered. As is well known, the photon distribution functions play an important role in the photoproduction of jets. The polarized distribution functions of the photon developed in Ref. 11 are used. Their important features are summarized in Section 3. In Sections 4 and 5, the results for the photoproduction of jets and heavy quarks are discussed, respectively. Finally, in Section 6 the conclusions are reviewed.

2. Distribution functions of the proton

The relevant quantities are the helicity difference distribution functions:

$$\Delta q_i(x_p, Q^2) = q_i^+(x_p, Q^2) - q_i^-(x_p, Q^2), \quad (1)$$

where $q_i^+(x_p, Q^2)$ ($q_i^-(x_p, Q^2)$) is the probability density for a quark of flavor i and momentum fraction x_p to have a helicity of the same (opposite) sign as

the helicity of the proton. The same expression applies for the anti-quarks and gluon. Q^2 is the QCD evolution scale. Assuming an SU(3) symmetric sea, the following parametrizations are used at $Q^2 = Q_0^2 = 4 \text{ GeV}^2$:

$$\begin{aligned}
x_p \Delta u_v(x_p, Q_0^2) &= N_{u_v} x_p^{a_{u_v}} (1 - x_p)^{b_{u_v}} (1 + \gamma_{u_v} x_p) \\
x_p \Delta d_v(x_p, Q_0^2) &= N_{d_v} x_p^{a_{d_v}} (1 - x_p)^{b_{d_v}}, \\
x_p \Delta s(x_p, Q_0^2) &= N_s x_p^{a_s} (1 - x_p)^{b_s}, \\
x_p \Delta c(x_p, Q_0^2) &= 0,
\end{aligned} \tag{2}$$

where

$$\begin{aligned}
N_{u_v} &= \Delta u_v(Q_0^2) / (\beta(a_{u_v}, b_{u_v} + 1) + \gamma_{u_v} \beta(a_{u_v} + 1, b_{u_v} + 1)), \\
N_{d_v} &= \Delta d_v(Q_0^2) / \beta(a_{d_v}, b_{d_v} + 1), \\
N_s &= \Delta s(Q_0^2) / \beta(a_s, b_s + 1),
\end{aligned} \tag{3}$$

$\beta(x, y)$ is the Euler beta function, and $\Delta q_i(Q_0^2)$ is the first moment of $\Delta q_i(x_p, Q_0^2)$:

$$\Delta q_i(Q_0^2) = \int_0^1 \Delta q_i(x_p, Q_0^2) dx_p. \tag{4}$$

All the quarks are assumed to be massless. Not enough experimental information is available to fit all the parameters, so that some phenomenological input has to be used. A strong constraint is provided by the requirement that the helicity difference distribution functions must be smaller than the corresponding unpolarized (helicity-sum) distribution functions. The parameters that are used satisfy this requirement with respect to the set DO1.1[12]. The small x_p behavior is fixed, following Altarelli and Stirling[6], by taking $a_{u_v} = a_{d_v} = 0.8$ and $a_s = 0.7$. The high x_p behavior is assumed to be similar to the behavior of the unpolarized distribution functions: $b_{u_v} = 3.7$, $b_{d_v} = 4.7$, and $b_s = 8$. Once an SU(3) symmetric sea is assumed, the normalization of

the valence quarks are fixed by the Bjorken sum rule and results from hyperon beta decay¹. Following Ref. 1, $\Delta u_v(Q_0^2) = 0.97$ and $\Delta d_v(Q_0^2) = -0.28$ are used. The sea normalization can be fixed with the EMC result on the spin dependent structure function:

$$g_1^p(x_p, Q^2) = \frac{1}{2} \sum_i e_i^2 (\Delta q_i(x_p, Q^2) + \Delta \bar{q}_i(x_p, Q^2)) \quad (5)$$

where e_i is the charge of q_i . Several groups have suggested that the difference between the Ellis-Jaffe [13] sum rule and the EMC result for the first moment of $g_1^p(x_p, Q^2)$ could be resolved by a larger higher

order correction due to a large gluon polarization[4, 14] or by a large sea contribution[5, 15](the sea contribution was set to zero in the Ellis-Jaffe sum rule). Several sets of helicity difference

distribution functions have been developed based on these ideas[6, 16]. However Bodwin and Qiu[10] showed that a hard gluonic contribution to the first moment of $g_1^p(x_p, Q^2)$ vanishes if an appropriate regularization scheme is used. Thus, the only way to resolve the discrepancy between the Ellis-Jaffe sum rule and the EMC result seems to be to assume a “large” negative sea contribution. This point of view is adopted here and $\Delta s(Q_0) = -0.11$ is taken. When the first moment of $g_1^p(x_p, Q^2)$ is estimated, the data are assumed to be Q^2 independent. The EMC result would prefer a somewhat larger a_s and larger negatively polarized sea when the x_p and Q^2 dependence are taken into account. However, as mentioned earlier, the unpolarized distribution functions give a strong constraint and limit $\Delta s(Q_0^2)$ to about the value it was assigned. Note that with these values for the parameters, the spin carried by the quarks is close to zero and, as was noted in Ref. 1, this still needs to be explained. The last parameter γ_{u_v} can be fit to reproduce the x_p and Q^2 dependence of $g_1^p(x_p, Q^2)$ measured by the EMC collaboration as well as possible. The result is $\gamma_{u_v}=2.54$. Because of the large sea contribution, there is no need for a large higher order correction, and a leading order analysis is suitable. This is consistent with the fact that later on in this paper leading order expressions are used. With this approach there is no experimental constraint on the helicity difference gluon distribution functions

¹Actually only the first moments need to be SU(3) symmetric for this to be true.

². The following parametrization is used:

$$x_p \Delta g(x_p, Q_0^2) = N_g x_p^{0.6} (1 - x_p)^8, \quad (6)$$

where

$$N_g = \Delta g(Q_0^2) / \beta(0.6, 1.8). \quad (7)$$

The value of the parameters are such that $\Delta g(x_p) \leq g(x_p)$ and that $\Delta g(Q_0^2) \sim 5$ is allowed. Three cases are considered: $\Delta g(Q_0^2) = .5, 3.0,$ and $5.7,$ respectively labeled set 1, 2, and 3. In Fig.1 both the helicity difference and unpolarized quark and gluon distribution functions are shown at $Q_0^2 = 4$ GeV for the three sets. The distribution can be obtained at another Q^2 by evolving them with spin-dependant Altarelli-Parisi equations[17]. In Fig.2 the EMC results, with statistical and systematic uncertainties added in quadrature are compared to the results of set 1 and 3, calculated at the appropriate Q^2 . The agreement between the data and the sets is good considering the fact that the sets are not the result of a fit of all the parameters. The difference between the two sets is due to the difference in the evolution of the sea quark helicity difference distribution functions.

In this section, three sets of helicity difference distribution functions were developed. At $Q^2 = Q_0^2$, they differ only in the size of the gluon polarization. As was pointed out, even the quark distribution functions are not well constrained yet. For the purpose of this paper, it is assumed that the quark distribution functions are fixed and the emphasis is on the sensitivity to the gluon helicity difference distribution function.

3. Distribution functions of the photon

As in the unpolarized case[18], an ‘‘asymptotic’’ solution can be derived from the spin-dependent Altarelli-Parisi evolution equations in the limit of large

²The constraint from evolution is small. The situation is similar to a leading order analysis of F_2^p in the unpolarized case.

momentum fraction (x_γ) and Q^2 . This is due to the direct coupling of the photon to quarks. In that asymptotic limit, the Q^2 dependence of the helicity difference distribution functions can be factorized:

$$\begin{aligned}\Delta q_i(x_\gamma, Q^2) &= \frac{\alpha}{2\pi} \ln\left(\frac{Q^2}{\Lambda^2}\right) \Delta h_i(x_\gamma), \\ \Delta g(x_\gamma, Q^2) &= \frac{\alpha}{2\pi} \ln\left(\frac{Q^2}{\Lambda^2}\right) \Delta h_g(x_\gamma),\end{aligned}\tag{8}$$

where α is the QED coupling constant and Λ the QCD constant. The Δh functions depend only on x_γ . The expression in Eq. 9 can be introduced in the spin-dependent Altarelli-Parisi evolution equations and the remaining x_γ dependent equations for the Δh can be solved numerically. This was carried out in Ref. 11 where a parametrization of the solution is provided ³. Four flavors and massless quarks were assumed. A solution valid at lower Q^2 and x_γ would require input distributions functions at a fixed Q^2 . Unfortunately, there are no experimental data to fix the parameters of these distribution functions, so the asymptotic solution is utilized for the entire Q^2 range under consideration. The same approach can be used in the unpolarized case and the parametrization of Ref. 19 is used here. In Fig. 3 both the polarized and unpolarized distribution functions are shown for up-type and down-type quarks. The distribution functions for the quarks are harder than in the proton case, as can be seen by comparing Fig. 1 and 3. This will favor configurations with high x_γ and low x_p . The polarized distribution function of the gluon is also shown in Fig. 3 even though at the energy considered in this paper, it doesn't play any role. Notice that at high x_γ the helicity difference distribution functions of the quarks are positive.

4. Two-jet production

Our goal is to study the sensitivity of the photoproduction of two jets to the gluon polarization. Both the photon and the proton are longitudinally

³At high x_γ the parametrization used for the quarks is bigger than the numerical result and the unpolarized distribution functions. Here, to correct for this, $\Delta q(x_\gamma) = q(x_\gamma)$ is used for $x_\gamma > 0.95$.

polarized. The photoproduction of two jets receive contributions from two classes of subprocesses. In the first class of subprocesses the photon interacts directly with the constituents of the proton (the “direct” contribution). In the second class, the photon interacts through its distribution functions (the “resolved” contribution). At leading order in perturbative QCD, the integrated cross section for the photoproduction of two jets is given by the following expression:

$$\sigma_{\gamma p \rightarrow 2jets}(s) = \sum_{a,b} \int_{\tau}^1 dx_{\gamma} f_{a/\gamma}(x_{\gamma}, Q^2) \int_{\tau_{\gamma}}^1 dx_p f_{b/p}(x_p, Q^2) \hat{\sigma}_{ab \rightarrow 2jets}(\hat{s}) \quad (9)$$

where $s = 2E_{\gamma}M_p$ is the square of the total energy available and $\hat{s} = x_{\gamma}x_p s$ is the square of the center of mass energy of the subprocesses. $f_{a/\gamma}(f_{b/p})$ is the distribution function of parton a(b) in the photon(proton). In the direct contribution case, $f_{a/\gamma}(x_{\gamma})$ is replaced by $\delta(1 - x_{\gamma})$. The choice of the scale Q^2 bears the usual ambiguity, $Q^2 = p_T^2/4$ is used. The sum is over all the possible subprocesses. The direct contribution is composed of two subprocesses: $\gamma q \rightarrow gq$ and $\gamma g \rightarrow q\bar{q}$. The resolved contribution is composed of eight subprocesses. The dominant subprocesses at the energy considered in this paper are $qq' \rightarrow qq'$ and $gq \rightarrow gq$. The lower limits of integration are given by the following expressions:

$$\begin{aligned} \tau &= \frac{4p_{Tmin}^2}{s} \\ \tau_{\gamma} &= \frac{4p_{Tmin}^2}{sx_{\gamma}} \end{aligned} \quad (10)$$

where p_{Tmin} is the minimum p_T of the jets. The matrix elements necessary to calculate the subprocess cross sections, $\hat{\sigma}$, can be found in Ref. 20 and 21. The integrated cross sections are presented in Table 1, at $E_{\gamma} = 200$ GeV and 400 GeV, and $p_{Tmin} = 3$ and 5 GeV. $E_{\gamma} = 200$ GeV corresponds to the average value for E_{γ} of present unpolarized experiments and 400 GeV is about the upper limit. $p_{Tmin} = 3$ GeV is the lowest value at which jets have

been observed in fixed target experiments[22]. $p_{T\min} = 5$ GeV is presented to show the variation of the different contributions with $p_{T\min}$. Both the direct and the resolved contributions are presented. The two contributions are furthermore divided into quark and gluon contributions corresponding to subprocesses involving a quark or a gluon inside the proton, respectively. The unpolarized case has already been study extensively [20, 23]. The important points are summarized briefly. As can be seen from Eq. 11, both the x_p and x_γ thresholds decrease when the energy increases or the $p_{T\min}$ decreases. As a result, the relative size of the gluon contribution (in both the direct and resolved contribution) and of the resolved contribution increases whenever the energy is increased or the minimum p_T decreased.

The integrated helicity difference cross section for the production of two jets is given by[9]:

$$(\sigma^{++} - \sigma^{+-})_{\gamma p \rightarrow 2jets}(s) = \sum_{a,b} \int_{\tau}^1 dx_\gamma \Delta f_{a/\gamma}(x_\gamma, Q^2) \int_{\tau_\gamma}^1 dx_p \Delta f_{b/p}(x_p, Q^2) \Delta \hat{\sigma}_{ab \rightarrow 2jets}(\hat{s}). \quad (11)$$

The first sign superscript in σ^{++} and σ^{+-} corresponds to the helicity of the photon, and the second to the helicity of the proton. The $\Delta f_{a/\gamma}$ and $\Delta f_{b/p}$ are the helicity difference distribution functions as defined in section 2 and 3. $\Delta \hat{\sigma}$ is the helicity difference cross section of the subprocess. The matrix elements for the different subprocesses can be found in Ref. 9 and 11. The longitudinal asymmetry can now be defined:

$$A_{ll} = \frac{\sigma^{++} - \sigma^{+-}}{\sigma^{++} + \sigma^{+-}}. \quad (12)$$

As usual, it is advantageous to consider a ratio because the theoretical and experimental uncertainties tend to cancel out. The results for the asymmetry of each of the contributions are shown in Table 2 for set 1 and 3 (smallest and largest gluon helicity difference distribution function), at the same energies and $p_{T\min}$ as in Table 1. An important property of the asymmetry is that it is a weighted average of the asymmetries of each of the contributions.

First, the direct contribution is considered. The quark contribution is dominated by the u_v quark because the cross section is proportional to the square of the charge of the quark, and the Δu_v is the largest of the quark helicity difference distribution functions. Both Δu_v and $\Delta \hat{\sigma}_{\gamma q \rightarrow gq}$ are positive so that the quark contribution gives a positive asymmetry. The difference between set 1 and set 3 for the quark contribution is small; it is due to the difference in evolution of the quark helicity difference distribution functions. For the gluon contribution Δg is positive and $\Delta \hat{\sigma}_{\gamma g \rightarrow q\bar{q}}$ is negative such that the asymmetry of this contribution is negative. As expected, there is a large difference between the results of the two sets in this case. At $E_\gamma = 200$ GeV and $p_{T\min} = 5$ GeV the difference between the asymmetry of the two sets for the gluon contribution is about 60%, whereas the difference for the total asymmetry is only about 15%. The large difference in the gluon contribution doesn't survive, because the size of the gluon contribution to the cross section is relatively small, see Table 1. For the other three cases in Table 2, the size of the gluon contribution is bigger and the difference between the two sets for the total asymmetry of the direct contribution is about 35 to 50%. Notice that it is important to consider the difference between the two sets, and not just the result of each set separately.

Second, the resolved contribution is studied. In this case, both the quark and gluon contributions give a positive asymmetry. As in the direct case, the difference between the two sets for the quark contribution is small. The difference between the two sets for the gluon contribution is not as big as in the direct case. This is due to the fact that the asymmetry of the leading subprocess ($gq \rightarrow gq$) is not as big, and that the helicity difference distribution functions of the photon had to be folded in. As a result, the difference between the two sets for the total asymmetry of the resolved contribution is at most 15%.

As can be seen in Table 2, the difference between the two sets for the total asymmetry is of the order of 10–15%. This difference is rather small compared to the range span by the gluon contribution of the direct contribution. The problem stems from the fact that the gluon contribution is negative in the direct case and positive in the resolved case, such that the two contributions partially cancel each other. An obvious way to improve upon this is to separate the direct and resolved contributions, and then use the direct contribution to measure the gluon polarization, as it is the most sensitive contribution. Eventually, the resolved contribution could be used

to study the quark helicity difference distribution functions of the photon. The same techniques developed for the unpolarized case can be implemented to separate the direct and resolved contributions. One way to do this is by tagging the remnant jet coming from the photon in the resolved case[24], another is by a complete reconstruction of the kinematics and an appropriate cut on x_γ [25].

More detailed information can be obtained by looking at the longitudinal asymmetries of the differential cross section. In Fig. 4 the x_p -distributions are presented at $E_\gamma = 200$ GeV and $p_{T\min} = 3$ GeV for the three sets developed in Section 2. In Fig. 4a the unpolarized cross section is presented for the direct (dashes) resolved (dots), and total (solid) contributions. The resolved contribution peaks at higher x_p to compensate for the lower x_γ . In Fig. 4b, 4c and 4d the asymmetry for the direct, resolved and total contributions, respectively, are plotted for the different sets (dashes: set 1, dots: set 2, solid: set 3). The weighting between the direct and resolved contribution to form the total contribution is well apparent. For each contribution, the largest difference between the three sets is at low x_p . Note that it is possible to reconstruct x_p only if both jets in the event are measured. In case this can not be done, the rapidity distribution of the jets in the γ -proton center of mass is shown in Fig. 5. Positive rapidity is in the direction of the incoming photon. The largest difference is at larger rapidity that corresponds to the lowest x_p . One could also look at the p_T distributions, and the difference between the sets is similar. For comparison, in Fig. 6 and Fig. 7 the same plots as in Fig. 4 and Fig. 5, respectively, are shown for $E_\gamma = 400$ GeV and $p_{T\min} = 3$ GeV.

5. Heavy Quark production

The formulas presented in Section 4 for the photoproduction of two jets are also valid for the photoproduction of an heavy quark pair. The only modification is the replacement of $p_{T\min}$ by m_q , the mass of the heavy quark, in Eq. 10. We will consider the production of the charm quark with $m_c = 1.5$ GeV. As is well known, the resolved contribution for the photoproduction of heavy quarks for the energy range considered here is of the order of a few percents, and can be neglected. For the direct contribution there is only one subprocess at leading order in perturbative QCD: $\gamma g \rightarrow Q\bar{Q}$, where Q stands

for a heavy quark. Assuming that there is no spin effect in the fragmentation of the charm into a D-meson, the Peterson fragmentation function can be used [26]:

$$D_c^D(z) = Nz(1-z)^2/((1-z)^2 + \epsilon z)^2 \quad (13)$$

where z is the momentum fraction of the D-meson, and N is taken such that $D_c^D(z)$ is normalized to 1. $m_D \sim m_c$ is assumed as in the derivation of Eq. 14. The parameter ϵ is taken at .15. The matrix elements needed to calculate the asymmetry were evaluated using the method described in Ref. 27. The results for the integrated cross section and the asymmetry are presented in Table 3, for sets 1 and 3. The difference between the asymmetries of the two sets is about 12% at $E_\gamma = 200$ GeV and 5% at $E_\gamma = 400$ GeV. These results are actually misleading. In Fig. 8 the p_T^2 -distribution of the D-meson along with the asymmetry distribution are presented for $E_\gamma = 200$ GeV. It is apparent that at low p_T where the mass terms dominate in the cross section, the asymmetry is positive, whereas at high p_T where the mass terms are not as important, the asymmetry is negative (as in the two jet production case). The difference between the sets is bigger than suggested by the integrated asymmetry. A better variable in this case to describe the difference between the sets is given by an “absolute” asymmetry, $|A|_u$, where instead of integrating the asymmetry at each phase space point with its sign, the absolute value at each point is integrated. The difference between the two sets for the absolute asymmetry give a measure of the biggest difference that can be reached. The results for $|A|_u$ are also shown in Table 3. The difference between the sets is of the order of 20% at $E_\gamma = 200$ GeV and 15% at $E_\gamma = 400$ GeV. The lower energy is favored in this case. In Fig. 9 and Fig. 10 the rapidity distribution and sum of the rapidity distributions (in case both D-mesons are reconstructed) are presented. As it is unlikely that the kinematics of the whole event can be reconstructed, the x_p distribution is not shown.

6. Conclusions

We have shown that both jets and heavy quark production in a photoproduction experiment can lead to a successful measurement of the gluon helicity difference distribution function. Considering the total asymmetry, the two jets and heavy quarks production cases have similar sensitivity. However, the small difference in the asymmetries between the different gluon polarizations (10–20%) might be a limiting factor. The best way to measure the gluon helicity difference distribution function is by using two jet production at low p_T , with separation of direct and resolved contribution. The direct contribution has the biggest sensitivity, with differences in the asymmetries of the order of 35–50%. The resolved contribution could be used to study the quark helicity difference distribution functions of the photon.

To conclude we emphasize that a direct measurement of the gluon helicity difference distribution function is important as it would clarify some of the theoretical debate.

Acknowledgements

One of us, S.K., acknowledge a useful discussion with J. Qiu, and thanks A. Stange for providing him with his package to numerically calculate helicity amplitudes and M. Doncheski for discussions about the polarized distribution functions. This research was supported in part by the Texas National Research Laboratory Commission and by the U.S. Department of Energy under contract number DE-FG05-87ER40319.

References

- [1] J.Ashman *et al.*, EMC collaboration, *Phys. Lett.* **206B** (1988) 364.
- [2] J.Ashman *et al.*, EMC collaboration, *Nucl. Phys.* **B328** (1989) 1.
- [3] For an overview see S. D. Bass and A. W. Thomas, CAVENDISH-HEP-92-5, ADP-92-1833-T115, SMC-92-25, Aug. 1992, and reference therein.

- [4] R. D. Carlitz, J. C. Collins, and A. H. Mueller, *Phys. Lett.* **214B** (1988) 229.
- [5] M. Gluck and E. Reya, *Z. Phys.* **C39** (1988) 569.
- [6] G. Altarelli and W. J. Stirling, *Particle World*, Vol 1, No 2, 40 (1989).
- [7] See for examples M. A. Doncheski and R. W. Robinett, *Phys. Rev.* **D46** (1992) 2011; M. Gluck and W. Vogelsang, *Phys. Lett.* **277B** (1992) 515; M. A. Doncheski and C. S. Kim, preprint MAD-PH-745, March 1993; and references therein.
- [8] Z. Kunszt, *Phys. Lett.* **218B** (1989) 243; M. Gluck, E. Reya and W. Vogelsang, *Nucl. Phys.* **B351** (1991) 579.
- [9] J. Babcock, E. Monsay and D. Sivers, *Phys. Rev.* **D19** (1979) 1483.
- [10] G. T. Bodwin and J. Qiu, *Phys. Rev.* **D41** (1990) 2755.
- [11] J. A. Hassan and D. J. Pilling, *Nucl. Phys.* **B187** (1981) 563.
- [12] J. F. Owens, *Phys. Lett.* **266B** (1991) 126.
- [13] J. Ellis and R. L. Jaffe, *Phys. Rev.* **D9** (1974) 1444; **D10** (1974) 1669 (E).
- [14] G. Altarelli and G. G. Ross *Phys. Lett.* **212B** (1988) 391; A. V. Elfremov and O. V. Teryaev, Dubna report E2-88-287 (1988), published in *Proceedings of the Int. Hadron Symposium*, Bechyne, Czechoslovakia, 1988, eds. X. Fisher *et al* (Czech. Academy of Science, Prague, 1989), p. 302.
- [15] J. Ellis, R. A. Flores and S. Ritz, *Phys. Lett.* **198B** (1987) 393 ; J. Ellis and R. A. Flores, *Nucl. Phys.* **B307** (1988) 883 ; M. Gluck and E. Reya, Univ. Dortmund report D)-TH 87/14 (1987).
- [16] C. Bourrely, J. ph. Guillet, and P. Chiappetta, *Il Nuovo Cimento*, **103A** (1990) 1337.
- [17] G. Altarelli and G. Parisi, *Nucl. Phys.* **B126** (1977) 298.

- [18] E. Witten, *Nucl. Phys.* **B120** (1977) 189.
- [19] D. W. Duke and J. F. Owens, *Phys. Rev.* **D30** (1984) 49.
- [20] J. F. Owens, *Phys. Rev.* **D21** (1980) 1980.
- [21] For the subprocesses of the resolved contribution see any good textbook, *e.g. Collider physics*, V. D. Barger and R. J. N. Phillips, Addison–Wesley Publishing company, Inc..
- [22] M. Corcoran, private communication.
- [23] H. Baer, J. Ohnemus, and J. F. Owens, *Phys. Rev.* **D40** (1989) 2844.
- [24] M. Drees, and R. M. Godbole, *Phys. Rev.* **D39** (1989) 169.
- [25] R. S. Fletcher, F. Halzen, S. Keller, and W. H. Smith *Phys. Lett.* **266B** (1991) 183.
- [26] C. Peterson, D. Schlatter, I. Schmitt, and P. M. Zerwas *Phys. Rev.* **D27** (1983) 105.
- [27] V. Barger A. L. Stange R. J. N. Phillips *Phys. Rev.* **D44** (1991) 1987.

Tables

E_γ (GeV)	$p_{T \min}$ (GeV)	direct			resolved			tot (nb)
		q-cont (nb)	g-cont (nb)	tot (nb)	q-cont (nb)	g-cont (nb)	tot (nb)	
200	5	10.2	3.2	13.4	2.5	1.2	3.7	17.1
200	3	103.	110.	213.	91.	110.	201.	414.
400	5	23.7	17.3	41.0	13.9	12.6	26.5	67.5
400	3	129.	217.	346.	231.	371.	602.	973.

Table 1: Integrated cross sections for dijet production averaged over the initial spins for different E_γ , and $p_{T \min}$.

set	E_γ (GeV)	$p_{T \min}$ (GeV)	direct			resolved			tot (%)
			q-cont (%)	g-cont (%)	tot (%)	q-cont (%)	g-cont (%)	tot (%)	
1	200	5	34.8	-7.9	24.7	10.1	3.4	7.9	21.1
3	200	5	34.9	-74.5	9.1	10.1	30.1	16.8	10.7
1	200	3	24.9	-8.3	7.8	2.8	2.6	2.7	5.3
3	200	3	24.9	-93.2	-36.0	2.8	29.	17.2	-10.1
1	400	5	28.4	-8.9	12.7	4.7	3.2	4.0	9.3
3	400	5	28.9	-89.2	-20.8	4.8	31.6	17.5	-5.7
1	400	3	18.0	-7.5	2.0	.9	1.8	1.4	1.6
3	400	3	18.2	-84.6	-46.4	.9	20.3	12.9	-8.7

Table 2: Asymmetries for dijet production for different sets of polarized distribution functions (set 1 and 3 of section 2), E_γ , and $p_{T \min}$.

proton set	E_γ (GeV)	cross section (nb)	A_{ll} (%)	$ A _{ll}$ (%)
1	200.	993.	1.2	2.2
3	200.	993.	13.2	23.6
1	400.	1475.	.5	1.5
3	400.	1475.	5.8	16.7

Table 3: Integrated cross sections and asymmetries for heavy quarks production for different sets of polarized distribution functions (set 1 and 3 of section 2), and E_γ .

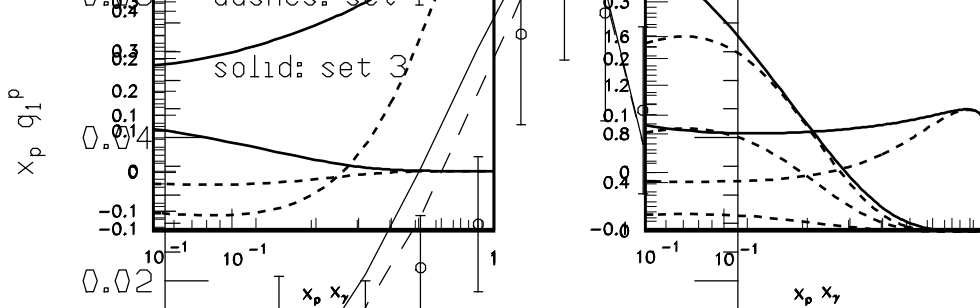


Figure 1: Unpolarized distribution functions (set DO1.1, solid) and helicity difference distribution functions (dashes) of the proton at $Q_0^2 = 4\text{GeV}^2$: a) valence up quark, b) valence down quark, c) sea quark, and d) gluon. In Fig. d) the 3 dashed curves correspond from the lowest to the highest to set 1, 2, and 3.

Figure 2: EMC result for the spin dependant structure function g_1^p as a function of x_p . Also shown are the results for set 1 (dashes) and set 3 (solid line), calculated at the appropriate Q^2 .

Figure 3: Unpolarized distribution functions (Ref. 19, solid) and helicity difference distribution functions (Ref. 11, dashes) of the photon at $Q_0^2 = 4\text{GeV}^2$: a) up type quark, b) down type quark, c) gluon.

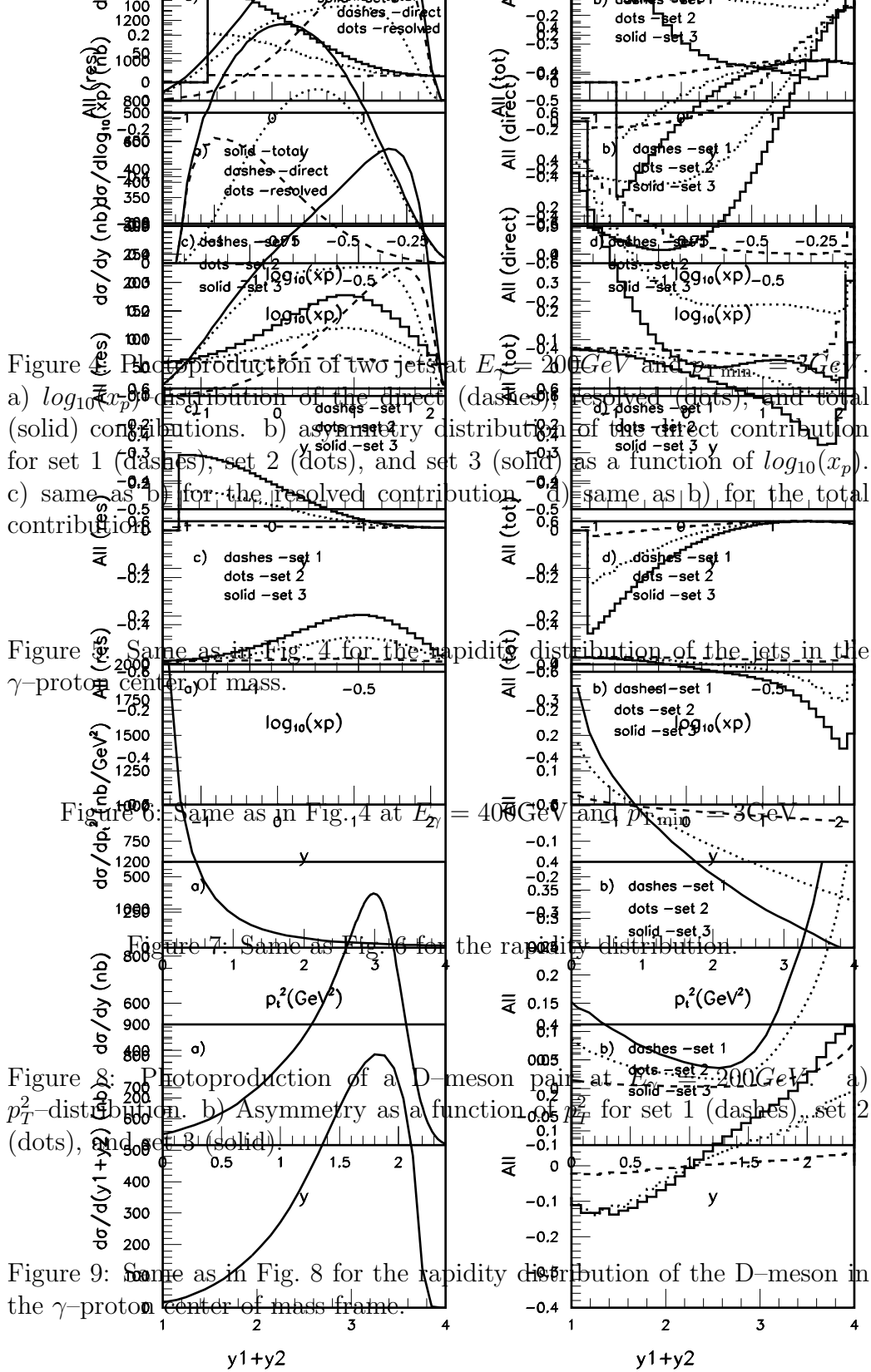


Figure 10: Same as in Fig. 8 for the rapidity-sum distribution.